ORGANIC MASS SPECTROMETRY, VOL. 24, 15–21 (1989)

Characterization of Cyclotrimethylenetrinitramine (RDX) by N,H Isotope Analyses with Pyrolysis–Atmospheric Pressure Ionization Tandem Mass Spectrometry

A. Peter Snyder†
US Army Chemical Research, Development and Engineering Center, SMCCR-RSL, Aberdeen Proving Ground, Maryland 21010-5423, USA

Johannes H. Kremer
Wehrwissenschaftliche Dienststelle der Bundeswehr für ABC-Schutz, Humboldtstrasse, D3042 Munster, FRG

Shirley A. Liebman
Geo-Centers, Inc., 10903 Indian Head Highway, Ft Washington, Maryland 20744, USA

Michael A. Schroeder and Robert A. Fifer
Ballistic Research Laboratory, Aberdeen Proving Ground, Maryland 21005-5066, USA

Pyrolysis–atmospheric pressure chemical ionization was used to study the thermal decomposition of the energetic material cyclotrimethylenetrinitramine (RDX) and characterization of the individual molecular ion products was accomplished by tandem mass spectrometry. The analysis was aided with pyrolysis mass spectra of the (^{15}N)- and perdeuterated RDX isotopes, and molecular formulae were derived for the *m/z* 46, 60, 74, 75, 85 and 98 molecular ions in the RDX pyrolysis mass spectrum. Equivalent fragments between the daughter ion mass spectra of the unlabeled and labeled RDX were determined in order to define a structure for each pyrolysis feature. Daughter ion mass spectra of pure reference compounds confirmed the identity of five of the six molecular ions. Perdeuterated RDX analyses provided evidence that *m/z* 74 and 75 are *N,N*-dimethylformamide and *N*-nitrosodimethylamine, respectively; *m/z* 46, 60 and 85 were identified as the protonated forms of formamide, *N*-methylformamide and dimethylaminoacetonitrile, respectively.

INTRODUCTION

Reaction rates and chemical mechanisms are two key topics that are fundamental to an understanding of the ignition/combustion process and product distribution of compounds used in propellants and explosives. Even more important are questions that address the thermodynamics, kinetic parameters and catalytic influences on the rate and end-product distributions in the ignition, combustion and detonation of solid propellants.[1] A structural analysis of the key fragments and intermediates resulting from the controlled heating of energetic compounds can yield important information relative to the understanding and enhancement of thermal processes. For this purpose, analytical pyrolysis/concentrator-gas chromatography was used to generate nitramine thermal decomposition profiles.[2–4] Furthermore, a large body of information exists on decomposition products of nitramines in the form of molecular formulae obtained by accurate mass measurements with high-resolution mass spectrometers.[5–8] However, few studies can be found that have produced direct, unambiguous analyses that delineate the structural identities of the end products.

Two compounds which are commonly used as ingredients in explosives and propellants are the nitramines cyclotrimethylenetrinitramine (RDX) and cyclotetranitramine (HMX). The former compound was chosen as a model for a structural analysis of the product molecular ions produced under oxidative pyrolysis–atmospheric pressure chemical ionization (Py–APCI) conditions.

Perdeuterated and (^{15}N)RDX were used in isotopic analyses of the key RDX mass spectral features, as well as collision-induced dissociation of the molecular ion products for comparison with daughter ion mass spectra of pure standard compounds. Some of the RDX

† Please send correspondence to: Commander, US Army Chemical Research, Development and Engineering Center, Attn: SMCCR-RSL/ A. Peter Snyder, Aberdeen Proving Ground, Maryland 21010-5423, USA.

Received 7 April 1988
Accepted 31 May 1988

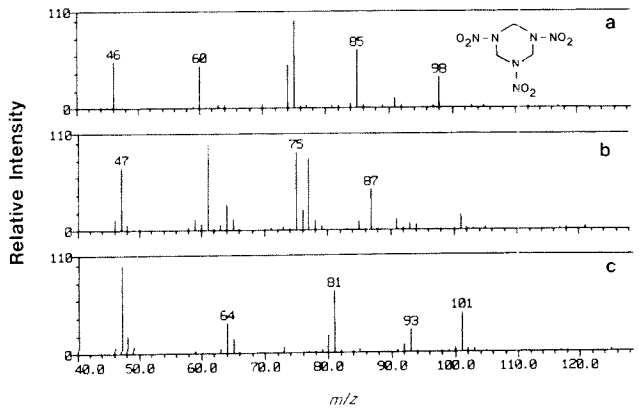

Figure 1. Py–APCI mass spectra of (a) RDX, (b) (^{15}N)RDX and (c) (^{2}H)RDX. The structure of RDX is shown as an inset in (a).

Py–APCI mass spectral features can be found in the Py–mass spectrometry literature for a number of important propellant ingredients.[5–12]

RESULTS AND DISCUSSION

Molecular formulae by isotope analyses

Figure 1(a) presents the Py–APCI mass spectra and structure of RDX. Molecular formulae and structural interpretations of the individual features in the Py–APCI mass spectrum of RDX are indeed formidable challenges. Therefore, isotopic analyses were performed in order to provide information to characterize each of the separate mass spectral features. Figure 1(b) and (c) depict the Py mass spectra of (^{1}H,^{15}N)RDX and (^{2}H,^{14}N)RDX, respectively. Note that Figs 1(a) and (b) show six main molecular ion features, but the perdeuterated RDX mass spectrum has only five main features. Table 1 summarizes the equivalent features for each of the RDX isotopes. For example, *m/z* 46 in Fig. 1(a) is observed as the *m/z* 47 ion in both (^{15}N)- and deuterium RDX isotopes, indicating that the *m/z* 46 feature contains one nitrogen and one hydrogen atom that originate from RDX. An *m/z* 74 analysis (Fig. 1 and Table 1) shows that it contains one nitrogen and seven hydrogen atoms, and a similar treatment with *m/z* 75 yields two nitrogen and six hydrogen atoms that originated from RDX.

Isotope analysis of each molecular ion from RDX produced a CHNO working formula (first column in Table 2) highlighting the number of hydrogen and nitrogen atoms that must be a part of the molecular ion and derived from RDX. The table of different CHNO molecular formulae for a given mass found in Silverstein *et al.*[13] was consulted for a tentative match to each of the six main features in the Py–APCI mass spectra. None of the molecular formulae in Silverstein *et al.*[13] contained HN combinations equivalent to the working formulae in Table 2 for each respective mass. Therefore, it was proposed that some of the RDX features were actually protonated forms of the working formulae. The protonated working formulae are listed in Table 2 and indeed, from Silverstein's tables,[13] *m/z* 74, 75, 85 and 98 each had only one molecular formula consisting of the respective number of RDX-derived hydrogen and nitrogen atoms with an extra proton. With this information, the number of carbon and oxygen atoms were automatically known for each formula, and the protonated molecular formulae for *m/z* 74, 75, 85 and 98 can be found in the last column of Table 2. However, *m/z* 46 and 60 did not result in similar analyses, hence the formula that had the least number of hydrogen atoms over that from the protonated working formula of the respective feature was chosen as a tentative molecular formula. These analyses of *m/z* 46 and 60 produced formulae of $[CH_3NO]H^+$ and $[C_2H_5NO]H^+$, respectively. Structural analysis of the six Py–APCI mass spectral features from RDX are detailed in the following discussion.

Table 1. Primary Py–APCI mass spectral features for RDX and corresponding signatures for the (^{15}N)- and (^{2}H)RDX isotopes (see Fig. 1)

RDX isotope	*m/z*					
^{14}N,^{1}H	46	60	74	75	85	98
^{15}N,^{1}H	47	61	75	77	87	101
^{14}N,^{2}H	47	64	81	81	93	101

Table 2. Determination of the molecular formula for each molecular ion in the RDX Py–APCI mass spectrum (Fig. 1(a))

m/z	Working formula[a]	Protonated working formula[b]	Molecular formula[c]
46	C_nHNO_x	$C_nH_2NO_x$	$[CH_3NO]H^+$
60	$C_nH_4NO_x$	$C_nH_5NO_x$	$[C_2H_5NO]H^+$
74	$C_nH_7NO_x$	$C_nH_8NO_x$	$[C_3H_7NO]H^+$
75	$C_nH_6N_2O_x$	$C_nH_7N_2O_x$	$[C_2H_6N_2O]H^+$
85	$C_nH_8N_2O_x$	$C_nH_9N_2O_x$	$[C_4H_8N_2]H^+$
98	$C_nH_3N_3O_x$	$C_nH_4N_3O_x$	$[C_3H_3N_3O]H^+$

[a] Derived from the isotope analysis in Table 1. The *n* and *x* subscripts are not necessarily the same values for each *m/z*.
[b] Protonated form of the working (isotope-derived) formula.
[c] Molecular formulae were derived by matching the protonated formula with each respective list of possible CHNO molecular formulae for a given *m/z* in Ref. 13.

***m/z* 46.** The perdeuterated RDX isotope mass spectrum (Fig. 1(c)) portrays a negligible amount of the *m/z* 46 feature. This leads to the elimination of nitrogen dioxide (NO_2) as a candidate for *m/z* 46 (Fig. 1(a)) in the positive ion mode. Furthermore, *m/z* 46 contains not only a nitrogen but also one hydrogen originating from RDX as is evident from the *m/z* 46 shift to *m/z* 47. It is well documented[6–8,12] that heating of RDX produces NO_2 under many different conditions and an intense *m/z* 46 feature has been observed in the negative ion mode under Py–APCI conditions (data not shown).

In the daughter ion spectra for *m/z* 46 and 47 (Fig. 2), it appears that *m/z* 18, 28 and 29 in the unlabeled com-

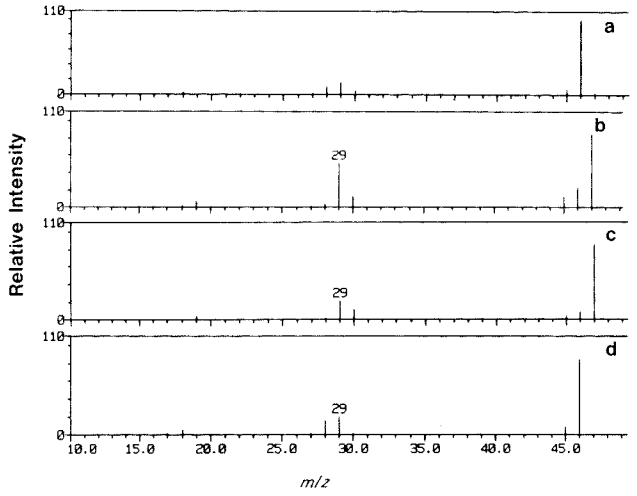

Figure 2. Py–APCI daughter ion mass spectra of (a) *m/z* 46, RDX, (b) *m/z* 47, (^{15}N)RDX, (c) *m/z* 47, (^{2}H)RDX, (d) *m/z* 46, protonated formamide.

pound (Fig. 2(a)) result in *m/z* 19, 29 and 30, respectively, for both ^{15}N and ^{2}H isotopes of RDX (Fig. 2(b) and (c)). No oxygen or carbon atom can be part of the *m/z* 18 feature because of the 1 u shift from *m/z* 18 to *m/z* 19 in both isotopes. This leads to the conclusion that NH_4^+ is the only possible structure, because (i) the nitrogen and one hydrogen atom originate from RDX and (ii) the other hydrogens must originate from the ion source. The 28 u fragment increases by 1 u for both RDX isotope species, which suggests the $[CNH]H^+$ and/or $[HCN]H^+$ ions, where one proton originates from RDX and the other is an ion source proton. The *m/z* 29 ion in Fig. 2(a) is observed to remain at *m/z* 29 in both isotope daughter ion mass spectra (Fig. 2(b) and (c)) and can be represented by the $[COH]^+$ fragment, where the liberated carbon monoxide is associated with a source proton. From this analysis, two possible structures with a molecular formula of CH_4NO can be considered: a protonated isocyanic acid derivative, $[OCNH_3]H^+$, or protonated formamide, $[HC(O)NH_2]H^+$.

Figure 2(d) shows the daughter ion mass spectrum of protonated formamide. In a comparison of Fig. 2(a) and (d), protonated formamide is indeed the *m/z* 46 feature in the Py mass spectrum of RDX. A paradox exists, because the proton (Fig. 1(a)) and deuterium (Fig. 1(c)) isotope analyses indicate only one RDX-derived hydrogen, while formamide contains three inherent protons. Possible explanations for this observation are that (i) free-radical hydrogen atom reactions could occur in the melt and/or gas phase and (ii) formation of HCN from RDX pyrolysis followed by hydrolysis with atmospheric/RDX decomposition-derived water and subsequent protonation in the ion source.

***m/z* 60.** An analysis of the daughter ion spectra of the *m/z* 60 molecular ion from RDX and its isotopes (Fig. 3(a)–(c)) reveals key fragments for this ion. A methyl function is obvious and *m/z* 28 consists of one nitrogen and one hydrogen from RDX (Fig. 3(d)). The *m/z* 28 fragment appears to be $[HCN]H^+$ where one hydrogen comes from RDX and the other is a source proton. The *m/z* 42 daughter ion feature contains one nitrogen and

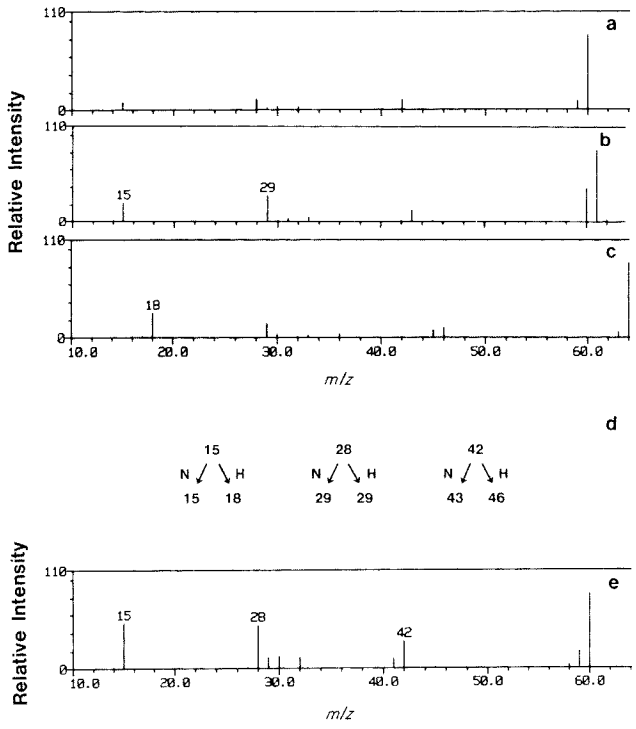

Figure 3. Py–APCI daughter ion mass spectra of (a) *m/z* 60, RDX, (b) *m/z* 61, (^{15}N)RDX, (c) *m/z* 64, (^{2}H)RDX, (e) *m/z* 60, protonated *N*-methylformamide. Figure 3(d) presents the *m/z* value for each major, unlabeled RDX daughter ion fragment and its equivalent fragment in the nitrogen (N) and hydrogen (H)-labeled RDX isotope.

four hydrogen atoms from the RDX molecule (Fig. 3(d)), and the $[H_3CN(H)C]^{+\bullet}$ and $[CH_3NCH]^{+\bullet}$ fragments appear to be logical candidates. A consistant 18 u difference appears between each respective primary molecular ion and highest mass daughter fragment, i.e. 60 – 42 (Fig. 3(a)), 61 – 43 (Fig. 3(b)) and 64 – 46 (Fig. 3(c)) and strongly suggests the presence of an oxygen atom. Possible candidates for *m/z* 60 can be $[H_3CNHC(O)H]H^+$, $[H_3CNCH]^{+\bullet}H_2O$ or a mixture of the two. Figure 3(e) shows the daughter ion mass spectrum from protonated *N*-methylformamide. A comparison of Fig. 3(a) and (e) shows that *m/z* 60 is indeed protonated *N*-methylformamide, $[H_3CNHC(O)H]H^+$. An explanation can be invoked for the presence of the two extra hydrogen atoms that is similar to that of the *m/z* 46 analysis.

***m/z* 74.** Figure 4(a)–(c) presents the *m/z* 74 daughter ion mass spectra of RDX and its isotopes. Because of the 1 u proximity of *m/z* 74 and 75 (Fig. 1(a)), daughter ion spectra of both species were obtained where the calibration of the *m/z* 73, $[H_2O]_4H^+$, reagent ion produced a baseline-to-baseline profile from *m/z* 72.5 to 73.5 and a peak width at half-height of 0.7 u. This procedure minimized daughter ion contribution of *m/z* 75 to the mass spectrum of *m/z* 74 and vice versa. The molecular formula of $[C_3H_7NO]H^+$ (Table 2) reveals that it is a protonated ion containing one nitrogen and one oxygen atom and seven hydrogen atoms originating from RDX. This molecular ion contains one more hydrogen than the RDX molecule itself, which strongly suggests inter-

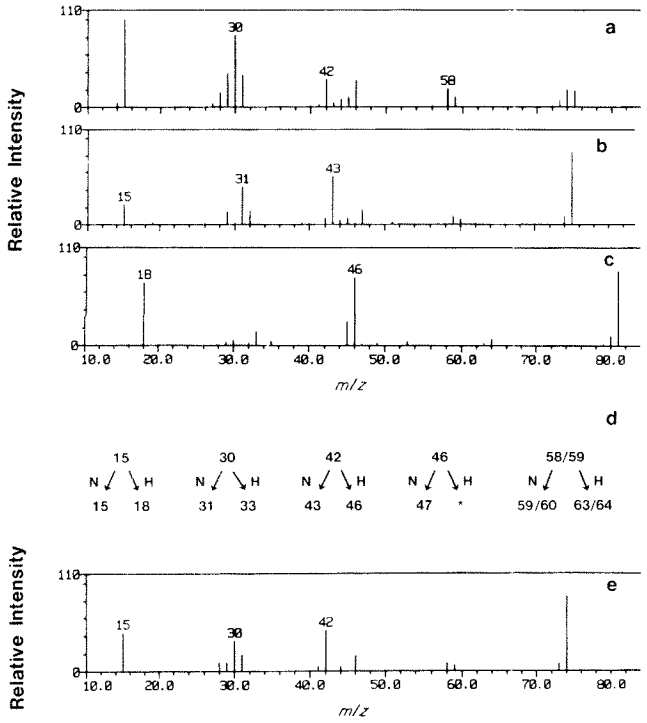

Figure 4. Py–APCI daughter ion mass spectra of (a) *m/z* 74, RDX, (b) *m/z* 75, (^{15}N)RDX, (c) *m/z* 81, (^{2}H)RDX, (e) *m/z* 74, protonated *N,N*-dimethylformamide. Refer to Fig. 3(d) for explanation of Fig. 4(d). (*) unclear *m/z* assignment.

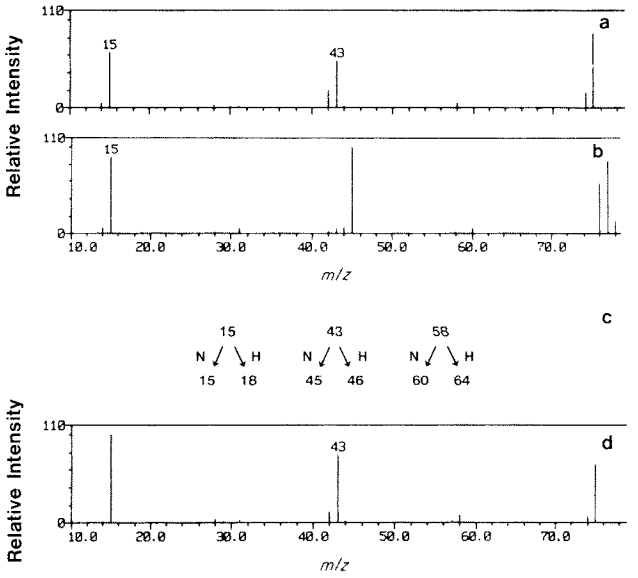

Figure 5. Py–APCI daughter ion mass spectra of (a) *m/z* 75, RDX, (b) *m/z* 77, (^{15}N)RDX, (d) *m/z* 75, protonated *N*-nitrosodimethylamine. Refer to Fig. 3(d) for explanation of Fig. 5(c).

molecular interactions in the melt state as well as reduction chemistry taking place during decomposition.

Figure 4(d) summarizes the daughter fragment ion distribution in Fig. 4(a)–(c), and it is clear that at least one methyl moiety is present. An *m/z* 30 analysis tentatively indicates a $[H_3CN]H^+$ moiety, and *m/z* 42 appears to be a $[H_3CNCH]^{+\cdot}$ fragment. Protonated carbon monoxide can account for the *m/z* 29 fragment (Fig. 4(a)–(c)). The *m/z* 46 feature appears to have one nitrogen (Fig. 4(d)); however, the (^{2}H)RDX mass spectral interpretation of this fragment is unclear (Fig. 4(c)). Figure 1(c) and Table 1 show that both *m/z* 74 and 75 in the unlabeled compound produce an *m/z* 81 feature in the perdeuterated sample. Therefore, structural interpretations of the unlabeled RDX *m/z* 74 and 75 species based on the perdeuterated derivative were interpreted with caution because of the two different *m/z* 81 molecular ions contributing to the same daughter ion mass spectrum (Fig. 4(c)). The $[H_3CCHNO]^{+\cdot}$ or $[H_3CNCHO]^{+\cdot}$ structures can account for the *m/z* 58 fragment while ether and hydroxy structural fragments were rejected.

Possible structures for *m/z* 74 include *N*-oxide compounds such as $[H_3CN(O)CHCH_3]^{+\cdot}$ or $[H_3CN(O)CH_2CH_3]^{+\cdot}$. However, because of the inherent charge on the former species, a source proton would not bind to it, and this interpretation would leave the molecular ion at *m/z* 73. The latter compound would be expected to yield an intense *m/z* 29 ethyl daughter ion fragment since NO is a good leaving group. The daughter ion mass spectrum of protonated *N,N*-dimethylformamide, $[(H_3C)_2NC(O)H]H^+$ (Fig. 4(e)), shows a satisfactory relationship with that of Fig. 4(a). Note that the *m/z* 74 ion is indeed composed of an *m/z* 73 molecular ion with an ion source proton attached to it (Table 2).

***m/z* 75.** Figure 5(a) and (b) presents the *m/z* 75 and 77 daughter ion mass spectra of (^{14}N)- and (^{15}N)RDX, respectively, and the isotope fragment analysis (Fig. 5(c)). The perdeuterated RDX mass spectrum of *m/z* 81 was already presented in Fig. 4(c). Relatively few daughter ion fragments are observed as compared to *m/z* 74. A methyl group is present, an *m/z* 43 analysis reveals $[NCHNH_2]^{+\cdot}$, $[HNCNH_2]^{+\cdot}$ and $[H_3CNN]^{+\cdot}$ as possible structures (Fig. 5(c)), and the features in the vicinity of *m/z* 30 were neglected owing to their low abundance. The *m/z* 58 fragment could be represented by the $[H_3CNCHNH_2]^{+\cdot}$, $[H_3CNHCNH_2]^{+\cdot}$ and $[(CH_3)_2NN]^{+\cdot}$ structures, and the remaining 17 u (to produce *m/z* 75) can come from an oxygen and ion source proton. Structures that best satisfy the daughter ion mass spectral information are $[H_3CN(O)CHNH_2]H^+$, $[H_3CNHC(O)NH_2]H^+$ and $[(CH_3)_2NNO]H^{+\cdot}$. An *m/z* 75 daughter ion mass spectrum of protonated *N*-nitrosodimethylamine $[(H_3C)_2NNO]H^+$ (Fig. 5(d)) was identical to that of *m/z* 75 in RDX (Fig. 5(a)). This structure is similar to that for *m/z* 74, with the formyl group being replaced by an NO group.

***m/z* 85.** The molecular formula as proposed in Table 2 is unusual in that it contains one carbon and two hydrogen atoms more than the RDX molecule itself (Fig. 1(a) inset). The daughter ion mass spectra of *m/z* 85 and the corresponding isotopic molecular ions are presented in Fig. 6(a)–(c). Figure 6(d) presents an analysis of each of the fragment ions in terms of equivalent, respective fragments for the unlabeled and labeled molecular ions.

At least one methyl group is observed and *m/z* 30 appears to be a $[H_3CN]H^+$ moiety with an ion source proton (Fig. 6(d)). The *m/z* 44 ion contains one nitrogen

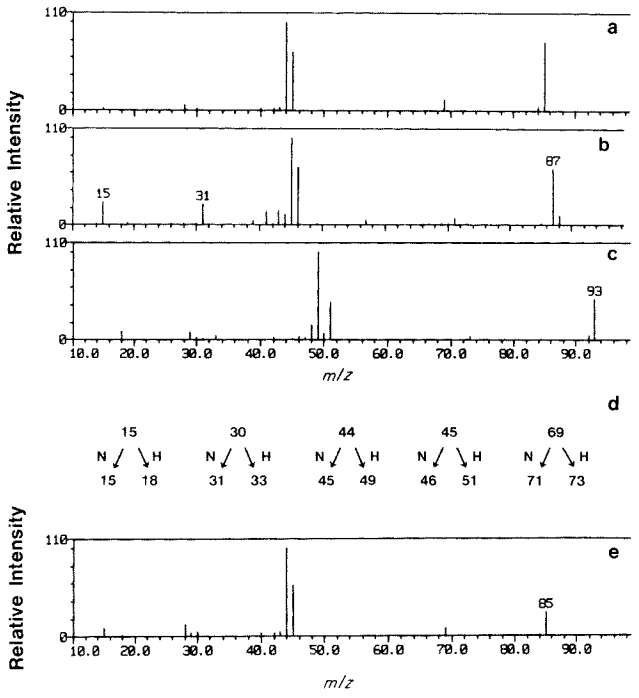

Figure 6. Py–APCI daughter ion mass spectra of (a) *m/z* 85, RDX, (b) *m/z* 87, (^{15}N)RDX, (c) *m/z* 93, (^{2}H)RDX, (e) *m/z* 85, protonated dimethylaminoacetonitrile. Refer to Fig. 3(d) for explanation of Fig. 6(d).

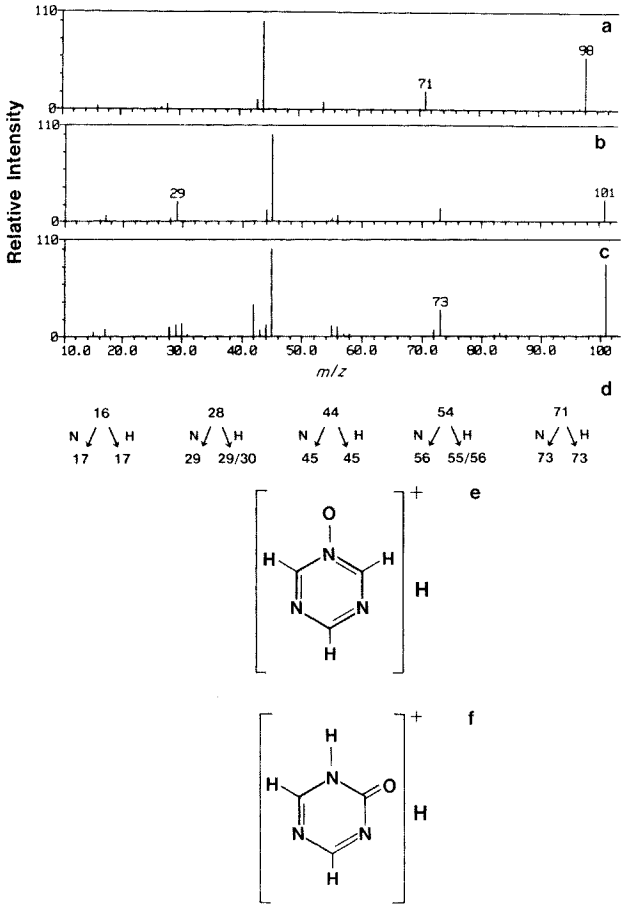

Figure 7. Py–APCI daughter ion mass spectra of (a) *m/z* 98, RDX, (b) *m/z* 101, (^{15}N)RDX, (c) *m/z* 101, (^{2}H)RDX. Refer to Fig. 3(d) for explanation of Fig. 7(d). (e), (f) Possible structures for *m/z* 98, RDX.

and five RDX-derived hydrogen atoms and appears to be any one of a number of fragments with a chemical formula of $[C_2H_5N]H^+$. The *m/z* 45 ion contains one nitrogen and six RDX-derived hydrogen atoms with structural permutations having the $[C_2H_6N]H^+$ chemical formula. The *m/z* 69 ion (Fig. 6(a)) contains two nitrogens and only four hydrogens derived from RDX and is 16 u apart from the molecular ion. This difference suggests an oxygen atom; however, this atom is not found in the protonated molecular formula (Table 2). Alternative sources of the 16 u loss are either a methyl group and source proton or an NH group with a source proton, $[NH]H^+$. With the aid of the isotopic analyses, a small suite of compounds was selected, and their daughter ion mass spectra were obtained. Protonated dimethylaminoacetonitrile, $[(CH_3)_2NCH_2CN]H^+$ (Fig. 6(e)) produced a better match with Fig. 6(a) than that of the other test compounds. Note that $(CH_3)_2NCH_2CN$ has one carbon and two hydrogen atoms more than RDX itself. This indicates that its formation is the result of intermolecular reactions among primary products and implies that reduction reactions are involved.

***m/z* 98.** The molecular ion $[C_3H_3N_3O]H^+$ (Table 2) consists of only three RDX-derived hydrogen atoms and strongly suggests a high degree of unsaturation in the molecule. Figure 7(a)–(c) presents the daughter ion mass spectra of *m/z* 98 and its nitrogen and hydrogen *m/z* 101 isotope equivalents. The methyl group is not observed, and *m/z* 28 appears to be protonated hydrogen cyanide as shown by the fragment analyses in Fig. 7(d). A structural analysis of the minor *m/z* 16 feature suggests the $[NH]H^+$ group. The *m/z* 44 ion is most likely protonated cyanic acid, $[HOCN]H^+$ or the isomeric structure $[HCNO]H^+$, and *m/z* 54, in consideration of the structure of RDX, can be the $[NCHNCH]^{+\cdot}$ fragment. Adding 17 u to the *m/z* 54 fragment would yield *m/z* 71, suggesting an oxygen/proton combination. Possible structures for this fragment can be $[CHNCHNO]H^+$, $[CHN(O)CHN]H^+$, $[NCHNCHO]H^+$ or $[NCH(O)NCH]H^+$ where the oxygen atom is located on an internal or external carbon or nitrogen atom.

To the best of the authors' knowledge, compounds with the chemical formula $C_3H_3N_3O$ are not commercially available, and therefore Fig. 7(e) and (f) presents two possible structures that best fit the isotope fragment analyses of *m/z* 98. Figure 7(e) is a protonated triazine-*N*-oxide and Fig. 7(f) represents an equivalent structure except that the oxygen is situated on a carbon atom. An inter- or intramolecular oxidation reaction could take place on the RDX molecule, which would lead to the proposed structures. The latter structure is a more attractive candidate in that it could act as a direct intermediate in the formation of the *m/z* 46 and 60 formamide-derived products.

Comparison of RDX mass spectral response with Py–APCI and thermal desorption electron ionization (EI) and chemical ionization (CI)

The chemical formulae and structural identities of the *m/z* 46, 74, 75, 85 and 98 features generated under

Py–APCI conditions are in contrast with many of the experimental findings in the literature.[5–7,9–12,14–21] Sample conditions such as field desorption[5] and direct insertion and solids probes with water, methane and isobutane CI[6,7,9,11,22–25] and EI[6,7,10,11] have yielded an *m/z* 74 feature that with accurate mass measurement (AMM)[6,7] corresponds to $[CH_2N_2O_2]^{+\cdot}$. In the above studies, nitroformimine, $[CH_2NNO_2]^{+\cdot}$, was proposed as the compound, and this species was also observed with infrared multiphoton dissociation of an RDX molecular beam.[26] AMM of *m/z* 75 produced a chemical formula of $[H_3CN_2O_2]^+$, and this species was rationalized as protonated nitroformimine. Spangler *et al.*[14] have shown that with flash evaporation of RDX on a solids probe in a heated atmospheric pressure ionization source a mass-identified ion mobility peak was found for *m/z* 75, and the authors assumed the identity of the ion was protonated nitroformimine. In the present report, however, under similar pyrolysis and ionization conditions, tandem mass spectrometry isotope analyses yielded the formamine and nitrosoamine derivatives for *m/z* 74 and 75, respectively.

RDX fragment analyses by EI and CI (~1 Torr) AMM have shown that *m/z* 46 and 85 are represented by the NO_2^+ and triazine ($C_3H_7N_3$), respectively.[2,6,7] In this study, atmospheric pressure thermolysis of RDX also yielded these mass spectral features; however, their identities are different in that protonated formamide and protonated dimethylaminoacetonitrile are responsible for the *m/z* 46 and 85 features, respectively. In addition to Py–APCI, thermal desorption EI and CI[6,7,10] and Knudson cell, molecular beam EI[21] of RDX have also produced the *m/z* 98 feature with an AMM-derived chemical formula of $[C_3H_4N_3O]^{+\cdot}$. A structural determination of *m/z* 98, however, is less definitive in that only protonated triazine oxide (Fig. 7(e)) has been proposed in the literature while the Py–APCI daughter ion analysis tends to support the carbon–oxygen analog in Fig. 7(f).

The type of thermal treatment (e.g. heating rate or maximum temperature), pressure (e.g. vacuum v. atmospheric) or ionization type (e.g. EI v. APCI) could potentially be responsible for the apparent differences in structures between this study and previous mass spectral studies of RDX. However, the conditions of this study favored ionized products from thermally induced fragments, while in most of the previous mass spectral studies of RDX the conditions were such that RDX was probably vaporized with little or no decomposition during the thermal treatment, then ionized, and subsequently fragmented by the excess internal energy imparted during the EI/CI process. Therefore, the thermal dissociation pathway and resulting products from the neutral RDX molecule may be different from those for the excited state ion. Further effort would be required to distinguish between condensed-phase and vapor-phase decomposition in our experimental arrangement.

CONCLUSIONS

Analytical Py–APCI was used to impose selected temperature and pressure conditions for the oxidative degradation of the energetic material RDX. Structural characterization of the pyrolysis products was achieved using (^{15}N)- and (^{2}H)RDX with triple quadrupole mass spectrometer instrumentation. Py–APCI tandem mass spectrometry thus revealed important insights into the decomposition of RDX under the selected experimental conditions. These studies emphasized thermally induced fragmentation processes and the transport of the resultant species into the APCI source. The combination of Py–atmospheric pressure ionization triple-quadrupole techniques with isotopically tagged samples was shown to be a powerful tool for structural elucidations and provided structural assignments that had not been reported in the previously cited mass spectrometric studies of RDX decomposition.

EXPERIMENTAL

A Sciex (Toronto, Canada) TAGA 6000 APCI triple-quadrupole mass spectrometer was used as the analyzer and detector for mass spectra collection. Background methods and general operating procedures for an APCI mass spectrometer system have been discussed by Dawson *et al.*[27,28] and the operating conditions for the present study can be found elsewhere.[3,29] Normal operating pressure in the conventional mass analyzer mode was 2.5–3.0 × 10^{-6} Torr, and all daughter ion analyses were obtained with a 6.0 × 10^{-5} Torr pressure of argon collision gas.

Pyrolysis of the solid samples was conducted with a Pyroprobe Model 122 controller (Chemical Data Systems, Oxford, Pennsylvania), with a platinum coil desorption probe. Pyrolysis was conducted with the temperature ramp (rise time) in the off position and the final set temperature was 360 °C. All runs used ~0.5–1.0 mg of powdered sample positioned in a quartz tube with quartz wool. The tube was placed into the desorption probe, and the latter was inserted into the ion source of the mass spectrometer. Details and a schematic of this interface are presented elsewhere.[3] All pyrolysis experiments were performed with an 80 cm^3 min^{-1} air flow from a compressed air cylinder (MG Industries, Valley Forge, Pennsylvania). Samples of (^{15}N)RDX and perdeuterated (^{2}H)RDX were obtained as gifts from S. Bulusu, Armament Research and Development Center, Dover, New Jersey. In preliminary experiments, all RDX samples were observed to contain acetone (*m/z* 59) in the pyrolysis mass spectra, and therefore they were vacuum-dried for one week to eliminate the solvent. Formamide, *N*,*N*-dimethylformamide, *N*-nitrosodimethylamine and dimethylaminoacetonitrile were obtained from Aldrich Chemical Co. Inc., Milwaukee, Wisconsin, and *N*-methylformamide was obtained from Eastman, Rochester, New York in high purity, and all were used without further purification. Mass spectral analysis of these liquid compounds were obtained by direct vapor sampling.

Acknowledgement

We thank Ms Linda Jarvis for the preparation and editing of the manuscript.

REFERENCES

1. R. A. Fifer, in *Fundamentals of Solid Propellant Combustion*, Vol. 90, Progress in Astronautics and Aeronautics Series, ed. by K. K. Kuo and M. Summerfield, pp. 201–237. American Institute of Aeronautics and Astronautics, New York (1984).
2. S. A. Liebman, P. J. Duff, K. D. Fickie, M. A. Schroeder and R. A. Fifer, *J. Hazardous Materials* **13**, 37 (1986).
3. S. A. Liebman, A. P. Snyder, J. H. Kremer, D. J. Reutter, M. A. Schroeder and R. A. Fifer, *J. Anal. Appl. Pyrolysis* **12**, 83 (1987).
4. S. A. Liebman and T. P. Wampler, in *Pyrolysis and GC in Polymer Analysis*, ed. by E. J. Levy and S. A. Liebman, Ch. 3. Marcel Dekker, New York, (1985).
5. H.-R. Schulten and W. D. Lehmann, *Anal. Chim. Acta* **93**, 19 (1977).
6. J. Yinon, D. J. Harvan and J. R. Hass, *Org. Mass Spectrom.* **17**, 321 (1982).
7. J. Yinon, *Mass Spectrom. Rev.* **1**, 257 (1982).
8. S. Bulusu and T. Axenrod, *Org. Mass Spectrom.* **14**, 585 (1979).
9. J. Yinon, *Biomed. Mass Spectrom.* **1**, 393 (1974).
10. J. Stahls, *J. Chem. Soc., Faraday Trans. 1* **67**, 1768 (1971).
11. P. Vouros, B. A. Petersen, L. Colwell, B. L. Karger and H. Harris, *Anal. Chem.* **49**, 1039 (1977).
12. M. A. Schroeder, Report No. AD-A159325, Ballistic Research Laboratory, Aberdeen Proving Ground, Maryland (1985).
13. R. M. Silverstein, G. C. Bassler and T. C. Morrill, *Spectrometric Identification of Organic Compounds*, Wiley, New York (1974).
14. G. E. Spangler, J. P. Carrico and S. H. Kim, in *Proceedings of the International Symposium on the Analysis and Detection of Explosives*, pp. 267–282. FBI Academy, Quantico, Virginia (1983).
15. M. A. Schroeder, Report No. AD-A160543, Ballistic Research Laboratory, Aberdeen Proving Ground, Maryland (1985).
16. M. A. Schroeder, in *Proc. 15th Joint Army–Navy–NASA–Air Force (JANNAF) Combustion Mtg*, Vol. II, pp. 17–34. Chemical Propulsion Information Agency (CPIA) Pub. No. 308, Rhode Island (1979).
17. M. A. Schroeder, in *Proc. 21st JANNAF Combustion Mtg*, Vol. II, pp. 595–614. CPIA Pub. 412, Rhode Island (1984).
18. J. N. Bradley, A. K. Butler, W. D. Capey and J. R. Gilbert, *J. Chem. Soc., Faraday Trans. 1* **73**, 1789 (1977).
19. M. Farber and R. D. Srivastava, *Chem. Phys. Lett.* **64**, 307 (1979).
20. S. Bulusu, *Org. Mass Spectrom.* **3**, 13 (1970).
21. R. Behrens, Jr, in *Proc. 23rd JANNAF Combustion Mtg.*, Vol. I, pp. 231–239. CPIA Pub. No. 457, Rhode Island (1986).
22. S. Zitrin and J. Yinon, *Adv. Mass Spectrom. Biochem. Med.* **1**, 369 (1976).
23. C. T. Pate and M. H. Mach, *Int. J. Mass Spectrom. Ion Phys.* **26**, 267 (1978).
24. R. G. Gillis, M. J. Lacey and J. S. Shannon, *Org. Mass Spectrom.* **9**, 359 (1974).
25. S. Zitrin, *Org. Mass Spectrom.* **17**, 74 (1982).
26. X. Zhao, E. J. Hintsa and Y. T. Lee, *J. Chem. Phys.* **88**, 801 (1988).
27. P. H. Dawson, J. B. French, J. A. Buckley, D. J. Douglas and D. Simmons, *Org. Mass Spectrom.* **17**, 205 (1982).
28. P. H. Dawson, J. B. French, J. A. Buckley, D. J. Douglas and D. Simmons, *Org. Mass Spectrom.* **17**, 212 (1982).
29. A. P. Snyder, J. H. Kremer, H. L. C. Meuzelaar, W. Windig and K. Taghizadeh, *Anal. Chem.* **59**, 1945 (1987).